The Cost of Risk-Aversion In Inventory Management

Angun, Ebru; Kleijnen, Jack

Publication date:
2024

Document Version
Early version, also known as pre-print

No. 2024-005

THE COST OF RISK-AVERSION IN INVENTORY MANAGEMENT: AN (s,S) CASE STUDY

By

Ebru Angün, Jack P.C. Kleijnen

5 March 2024

ISSN 0924-7815
ISSN 2213-9532

The cost of risk-aversion in inventory management: an (s, S) case study

Ebru Angün (a) and Jack P.C. Kleijnen (b)
(a) Industrial Engineering Department
Galatasaray University
Istanbul, Turkey
E-mail: eangun@gsu.edu.tr
Orcid: https://orcid.org/ 0000-0002-8199-9746
(b) Department of Management
Tilburg School of Economics and Management
Tilburg University
Postbox 90153, 5000 LE Tilburg, Netherlands
E-mail: kleijnen@tilburguniversity.edu
Orcid: https://orcid.org/0000-0001-8413-2366

March 4, 2024

Abstract

To model a risk-averse attitude (instead of a risk-neutral attitude), we may require that the 90% quantile (instead of the expected value) of a specific uncertain (or random) response satisfy a prespecified threshold which corresponds with a chance constraint. We include a case study; namely, an (s, S) inventory model that is specified in the literature. In this study we require that the 90% quantile of the service level exceed a prespecified threshold. So, we need to estimate the optimal values of s and S, which satisfy this service-level constraint while minimizing the expected inventory cost. To solve the resulting constrained optimization problem, we apply a recent variant of "efficient global optimization" (also known as "Bayesian optimization" and related to "active" machine learning). Our numerical results for the case study imply that the mean inventory cost increases by 2.4% if management is risk-averse instead of risk-neutral.

Keywords: risk aversion, chance constraint, inventory management, simulation optimization

JEL: C0, C1, C9, C15, C44

1 Introduction

In this paper, we investigate the financial consequences if managers are *risk-averse* instead of *risk-neutral,* in their control of inventory systems. We model this risk attitude through *quantiles* that characterize the tail of the *probability density function* (PDF) of the disservice level; this level is the complement of the service level (it is mathematically convenient to measure the disservice level instead of the service level, as we shall see in (3); quantiles are also used to quantify "value at risk" in financial portfolio management).

We let w_1 denote the percentage (or fraction) of customers that experience a *stockout* or disservice, per period (e.g., per day). The *90% quantile* of w_1—denoted by $q_{0.90}(w_1)$—implies that the probability is at least 90% that this percentage does not exceed $q_{0.90}(w_1)$. We assume that the managers are *risk-neutral* regarding the relevant *inventory cost*—denoted by w_0—which excludes the hard-to-quantify cost of out-of-stock, so we use a service-level constraint. Altogether, our goal is to minimize $E(w_0)$ (expected value or mean of w_0), while satisfying the constraint $q_{0.90}(w_1) \leq c_1$; e.g., $c_1 = 0.10$. Our formulation with quantile constraints also covers probabilistic or chance constraints; see (4). (Another example of quantiles in inventory management is a warehouse with a capacity c where the selected quantile of the physical inventory PDF should not exceed this c.)

The precise definition of the *service level* is a moot issue; e.g.,

https://en.wikipedia.org/wiki/Service_level (edited 22 February 2022)

states "Several definitions of service levels are used in the literature as well as in practice. These may differ ... with respect to the time interval they are related to". That website includes a definition of "β service level (type 2)", which agrees with our definition. Furthermore, Bashyam and Fu (1998) discusses various definitions; we use the definition selected in that article. Chen and Thomas (2017, Table 1) also discusses different definitions. Maitra (2024) uses a "cumulative demand fill rate".

We assume that management controls the inventory through the popular (s, S) *model*; i.e., a new order is placed as soon as the *inventory position*—defined as on-hand stock minus backorders plus outstanding orders—decreases below the *reorder level* s, and the size of this order is such that the inventory position increases to the *order-up-to level* S. Additionally, we assume that the inventory is *monitored per period* (e.g., per day) p with $p = 1, 2, ..., P$ where P denotes the end of the evaluation. To find the optimal s and S when orders may cross in time, we need to apply simulation. Obviously, P *terminates* the simulation run. Furthermore, we assume *identically and independently distributed* (IID) *demand* in period p—denoted by D_p—and IID *lead time* L. Both D_p and L have known PDFs with known parameters, so, this model does have *aleatory* uncertainty, but no *epistemic* uncertainty; these two types of uncertainty are detailed in Kleijnen (2015). Finally, we assume that $P = 30{,}000$ gives *steady-state* (stationary or long-run) outputs For more details on the assumed (s, S) model we refer to Bashyam and Fu (1998).

In practice, (s, S) models—for a single article or *stock-keeping unit* (SKU)—

are major *building blocks* for inventory management with multiple SKUs and production-inventory supply networks.

Obviously, risk-aversion implies that $E(w_0)$ increases when satisfying (say) $q_{0.90}(w_1) \leq 0.10$ instead of $E(w_1) \leq 0.10$. However, it is not obvious how much $E(w_0)$ increases; i.e., how much s and S change, and what the effect is on $E(w_0)$. It is well known that the optimal selection of s and S—given a service level constraint—is a hard mathematical problem; we summarize some solution methods.

Kleijnen et al. (2023) combines the popular *efficient global optimization* (EGO) algorithm—which is closely related to *Bayesian optimization* (BO) and *machine learning* (ML), especially *active learning*—and the *Karush-Kuhn-Tucker* (KKT) conditions—which are well-known (first-order necessary) optimality conditions in *mathematical programming* (MP), but are not used in other EGO methods. More precisely, EGO uses Kriging or *Gaussian process* (GP) "meta-models" (approximations, emulators, surrogates) of simulation models. EGO is a rapidly evolving field.

Whereas Kleijnen et al. (2023) assumes *deterministic* simulation, Angün and Kleijnen (2023) assumes *random* or *stochastic* simulation with outputs that are means (not quantiles). We shall summarize Angün and Kleijnen (2023)'s algorithm—which we call EGO-KKT—and apply it to our (s, S) model with a service-level constraint involving a quantile.

Maitra (2024) solves a related optimization problem—in a stochastic system dynamics model of inventory management—via BO, but uses neither quantiles nor the KKT conditions. Ouyang et al. (2023) uses *stochastic Kriging* (SK) as Angün and Kleijnen (2023) does, but does not use EGO or BO for the optimization of an (s, S) model without a service-constraint; i.e., this model assumes known out-of-stock cost. Coelho and Pinto (2018) applies EGO—using *ordinary Kriging* (OK)—to minimize the mean (not a quantile) response time of a medical emergency system by allocating ambulances to several city bases.

The main result of our (s, S) case study is that $E(w_0)$ increases by 2.4% if management is risk-averse (modeled by $q_{0.90}(w_1)$) instead of risk-neutral (modeled by $E(w_1)$).

We organize the rest of this paper as follows. Section 2 reviews related recent literature. Section 3 details the mathematical formulation of our inventory problem, and its solution via Angün and Kleijnen (2023)'s EGO variant. Section 4 gives numerical results for the simulation optimization of our (s, S) model with a constraint for either $E(w_1)$ or $q_{0.90}(w_1)$. Section 5 summarizes our conclusions and possible future research topics.

2 Literature review

We summarize some recent publications on quantiles of simulation output. These quantiles are frequently used as *risk* measures for different types of problems such as our simulation optimization problems and input uncertainty (or epistemic) problems discussed in Parmar et al. (2022) and Song et al. (2024).

(We do not discuss publications—such as Lu and Paulson (2023)—that use quantiles of the infill criterion, which is used to select input combinations to be simulated; see (12).)

Chang (2015) considers unconstrained optimization of a quantile, including optimal order quantities of multiple SKUs while assuming known back-order penalty cost. That publication does not use EGO. Chang (2015) is extended in Chang and Lu (2016), adding deterministic output constraints solved by penalty functions (whereas we allow random output constraints and use EGO combined with a penalty function that measures how well the KKT conditions hold). Chang (2016a) further extends Chang (2015), adding constraints for quantiles—while another quantile is minimized—and deterministic constraints for inputs. Chang (2016b) considers a deterministic simulation model with inputs sampled from given PDFs. Chang and Cuckler (2022) develops a simulation optimization method that minimizes a specific quantile (e.g., the 95% quantile) while satisfying an upper bound for the total cost which is assumed analytically available. That publication applies that method to solve vehicle fleet sizing for an automated material handling system in a wafer fab in Taiwan, minimizing a specific quantile of transport time of wafer lots; obviously, this fleet sizing implies integer (instead of continuous) variables. The method does not use EGO. Chang and Lin (2023) includes a chance constraint in a simulation-optimization method for system reliability via the allocation of redundant system components (obviously, the number of components is an integer); that method does not use EGO.

Hu et al. (2022) considers unconstrained optimization of a quantile in investment portfolio simulation (instead of inventory simulation), but that publication does not estimate these quantiles and their derivatives through Kriging.

Wang et al. (2022) discusses some algorithms for *un*constrained optimization of loss functions. These algorithms should not require strict properties for the loss functions such as convexity, and should allow computationally expensive simulations. Therefore that article uses metamodels; namely Kriging models.

Baker et al. (2022, Section 3.3.1) briefly discusses output quantiles, in a review of Kriging for analyzing stochastic simulation.

Kleijnen (2015, p. 208) gives additional references for Kriging of quantiles.

3 Mathematical problem formulation

Section 3.1 discusses quantiles in our (s, S) simulation model. Focusing on these quantiles, Section 3.2 summarizes constrained optimization. Section 3.3 summarizes Kriging. Section 3.4 summarizes EGO combined with KKT conditions.

3.1 An (s, S) simulation model with a quantile constraint

Following Bashyam and Fu (1998, eq. 3), we define Y_p as the *stockout* (demand not satisfied from on hand stock) in period p and we estimate the *disservice*

level through the running *average* of P' periods:

$$w_{1;P'} = \frac{\sum_{p=1}^{P'} Y_p}{\sum_{p=1}^{P'} D_p} \text{ with } P' = 1, ..., P = 30,000. \quad (1)$$

Note: Because $E(D_p)$ is a known input, an alternative *estimator* replaces the denominator in (1) by $P' \times E(D_p)$; however, we do not know whether this alternative estimator has a smaller *mean squared error* (MSE). An alternative *definition* of the service level replaces the right-hand side in (1) by $\Sigma(Y_p/D_p)/P'$, which turns out to give lower observations on $w_{1;P'}$.

We let $F(w_1)$ denote the marginal *cumulative density function* (CDF) of $w_{1;P'}$ (serial correlations among $w_{1;P'}$ do affect the joint CDF, but not the marginal CDF in the steady state). Then the standard definition of the $(1-\alpha)$ *quantile* of w_1 is

$$q_{1-\alpha}(w_1) = F^{-1}(1-\alpha) = inf\ [w_1 : F(w_1) \geq 1-\alpha]; \quad (2)$$

see Alexopoulos et al. (2019, p. 1162) and Lolos et al. (2023), which give more references.

Whereas Bashyam and Fu (1998) uses $E(w_{1;P'})$ with $P' \uparrow \infty$ and the estimator $w_{1;P'}$ with $P' = P = 30{,}000$, we use $q_{1-\alpha}(w_1)$ and the estimator $\widehat{q}_{1-\alpha}(w_1)$—computed as follows. We sort the P' observations $w_{1;P'}$ in ascending order, so $w_{1;(1)} \leq w_{1;(2)} \leq ... \leq w_{1;(P'-1)} \leq w_{1;(P')}$; i.e., we use the *order statistic* $w_{1;(\lceil (1-\alpha)P' \rceil)}$ (where $\lceil x \rceil$ denotes the ceiling function of the real number x), so, $\alpha = 0.10$ and $P' = 30{,}000$ gives $\widehat{q}_{1-\alpha}(w_1) = w_{1;(27000)}$. This popular quantile estimator is also used in Alexopoulos et al. (2019), focusing on *confidence intervals* (CIs) for quantiles based on a single replication, whereas we use multiple replications—as we shall see below (Section 3.3).

The upper part of Fig. 1 displays the estimated PDF (or histogram) of $w_{1;P'}$ that uses 100 bins, for $P' = 1$, ..., 30,000, in a specific simulation replication. We start (initialize) this replication with an on-hand (physical) inventory of S units and $S = 1{,}247.8$ and $s = 1{,}161.9$ (these specific values for s and S are the estimated optimal values in Angün and Kleijnen (2023), using the constraint $E(w_1) \leq 0.10$ instead of $q_{1-\alpha}(w_1) \leq 0.10$). This histogram shows $w_{1;P'} = 0$ for a few P'-values (actually, these values occur in the initial phase, because the simulation starts with a high physical inventory, zero backorders $Y_{P'}$, and zero outstanding orders; it turns out that $Y_{P'} = 0$ for $P' = 1$, ..., 21).

The lower part of Fig. 1 displays the estimated CDF or *empirical density function* (EDF), which makes jumps at the values of $w_{1;(P')}$; because some $w_{1;(P')}$-values turn out to be the same, some jumps are higher than 1/30,000. This plot implies (for example) $\widehat{q}_{0.80} = 0.1158$, $\widehat{q}_{0.90} = 0.1171$, $\widehat{q}_{0.95} = 0.1178$, and $\widehat{q}_{0.99} = 0.1226$. To eliminate the initial, transient phase, we might delete the first observations on $w_{1;P'}$; however, we find that eliminating the first 30 observations changes only the fourth decimal of $\widehat{q}_{0.80}$, $\widehat{q}_{0.90}$ and $\widehat{q}_{0.95}$ and the third decimal of $\widehat{q}_{0.99}$.

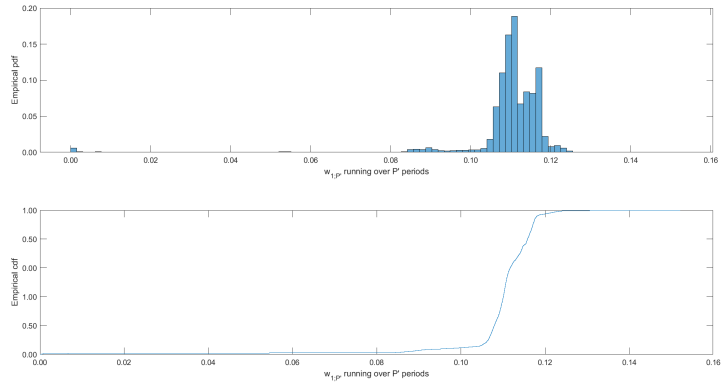

Figure 1: Running average of disservice fraction after P' periods with $P' = 1$, ..., 30,000: PDF and CDF

3.2 Optimization with a constrained quantile

Whereas Angün and Kleijnen (2023) investigates *general* constrained optimization problems with simulation estimates of means instead of quantiles, we focus on a specific (s, S) simulation model with the goal output $E(w_0)$, denoting the mean cost (see Section 1) and the constrained output $q_{0.90}(w_1)$ denoting the 90% quantile of the disservice fraction (see Section 3.1). Let c_1 denote the *upper threshold* for $q_{0.90}(w_1)$. Let $\boldsymbol{x} = (x_1, x_2)'$ denote the $k = 2$ *control* or *decision* variables $x_1 = s$ and $x_2 = Q$ with $Q = S$ - s; it is convenient not to use $x_2 = S > s$ (see Section 4 on our numerical experiments). Finally, we use the popular *box constraints* $l_j \leq x_j \leq u_j$ for the (deterministic) inputs x_j, which determine the *experimental area*. Altogether, we wish to solve the following *constrained optimization problem*:

$$\begin{gathered} \min_{\boldsymbol{x}} E[w_0(\boldsymbol{x})] \text{ subject to} \\ q_{1-\alpha}[w_1(\boldsymbol{x})] \leq c_1 \\ \boldsymbol{l} \leq \boldsymbol{x} \leq \boldsymbol{u} \text{ with } \boldsymbol{l} = (l_1, l_2)', \boldsymbol{u} = (u_1, u_2)'. \end{gathered} \tag{3}$$

This problem formulation also covers *chance constraints*:

$$\text{Prob}[w_1(\boldsymbol{x})] \leq c_1] \geq 1 - \alpha \iff q_{1-\alpha}[w_1(\boldsymbol{x})] \leq c_1. \tag{4}$$

However, a practical simulation model is a *black box*; i.e., $E[w_0(\boldsymbol{x})]$ and $q_{1-\alpha}[w_1(\boldsymbol{x})]$ in (3) are unknown *input/output* (I/O) functions. Consequently, we do not know whether this problem is non-convex (with multiple optima) or convex (with a single optimum). Like many authors, we estimate these functions through Kriging (meta)models, which give explicit approximations of the implicit I/O functions defined by the underlying simulation model. More

details on Kriging are given in Kleijnen (2015, p. 284). For our problem defined in (3) we use specific Kriging models, as follows.

3.3 Kriging

Like most publications on Kriging/GP in EGO/BO, we apply *univariate Kriging* instead of multivariate Kriging or *co-Kriging*; i.e., we ignore the correlations between different types of simulation outputs (in our case study, the correlation between $w_0(\boldsymbol{x})$ and $w_1(\boldsymbol{x})$; obviously, $\widehat{q}_{(1-\alpha)}[w_1(\boldsymbol{x})]$ depends on $w_1(\boldsymbol{x})$). Because the (s, S) simulation is stochastic instead of deterministic, we apply SK instead of OK. We use the—rather complicated—formulas for the *SK* predictor $\widehat{y}$ and its variance $s^2(\widehat{y})$ that are derived in Ankenman et al. (2010) (this $\widehat{y}$ and Y_p in (1) denote different random variables). These formulas assume $m_i > 1$ *replications* for the *old* simulated input combination $\boldsymbol{x}_i$ ($i = 1, ..., n$ where n is selected via (8)). Obviously, these replications have a common fixed simulation-runlength $P = 30{,}000$, and they use non-overlapping streams of *pseudorandom numbers* (PRN). These replications give the m_i IID outputs $w_{0;r}(\boldsymbol{x}_i)$ and $\widehat{q}_{(1-\alpha);r}[w_1(\boldsymbol{x}_i)]$ with $r = 1, ..., m_i$. For SK, we find it convenient to denote these two outputs by $o_{0;r} = w_{0;r}$ and $o_{1;r} = \widehat{q}_{1-\alpha;r}(w_1)$. Obviously, these m_i replications give the averages

$$\overline{o}_h(\boldsymbol{x}_i) = \frac{\sum_{r=1}^{m_i} o_{h;r}(\boldsymbol{x}_i)}{m_i} \; (h = 0, 1) \; (i = 1, ..., n) \tag{5}$$

and the (classic) unbiased estimators of the (heterogeneous) variances

$$s^2[o_h(\boldsymbol{x}_i)] = \frac{\sum_{r=1}^{m_i}[o_{h;r}(\boldsymbol{x}_i) - \overline{o}_h(\boldsymbol{x}_i)]^2}{(m_i - 1)}; \; s^2[\overline{o}_h(\boldsymbol{x}_i)] = \frac{s^2[o(\boldsymbol{x}_i)]}{m_i}. \tag{6}$$

SK assumes that the so-called *intrinsic noise*—caused by the PRN—has a Gaussian (or normal) distribution with zero mean and heterogeneous variances. We apply SK to $\overline{w}_0(\boldsymbol{x}_i)$ and $\overline{\widehat{q}}_{1-\alpha}[w_1(\boldsymbol{x}_i)]$, which are averages of m_i IID observations $w_{0;r}$ and $\widehat{q}_{(1-\alpha);r}[w_1(\boldsymbol{x}_i)]$ so we assume that the *central limit theorem* (CLT) applies; i.e., we assume that $\overline{w}_0(\boldsymbol{x}_i)$ and $\overline{\widehat{q}}_{1-\alpha}[w_1(\boldsymbol{x}_i)]$ are normally distributed. We denote the intrinsic noise by $e_{h;r}(\boldsymbol{x}_i)$—or briefly $e_{i;h;r}$—and its average by $\overline{e}_h(\boldsymbol{x}_i)$—or $\overline{e}_{i;h}$. Let $\boldsymbol{\Sigma}_{\overline{e};h}$ denote the *covariance matrix* of $\overline{e}_{i;h}$. Like most publications on SK, we do not apply *common random numbers* (CRN) so $\boldsymbol{\Sigma}_{\overline{e};h}$ is an $n \times n$ *diagonal* matrix. We define $\widehat{\boldsymbol{\Sigma}}_{\overline{e};h}$ as the corresponding matrix with the main-diagonal elements $s^2[\overline{o}_h(\boldsymbol{x}_i)]$ (defined in (6)).

Besides intrinsic noise, Kriging (including SK) considers *extrinsic noise* which models how the Kriging outputs—of a given type h—at two points $\boldsymbol{x}$ and $\boldsymbol{x}'$ are more correlated, the "closer" $\boldsymbol{x}$ and $\boldsymbol{x}'$ are—which is a realistic assumption if the simulation output functions are smooth. This noise implies that a Kriging model is a stationary GP or a *multivariate normal distribution* with a specific covariance matrix. This covariance matrix is determined by the specific type of correlation function that is selected; we select the popular *Gaussian* or *squared*

exponential correlation function with the so–called *length-scale hyperparameters* $\boldsymbol{\theta}_h = (\theta_{h;1}, ..., \theta_{h;k})'$ where $\theta_{h;j} \geq 0$:

$$\rho(\boldsymbol{\theta}_h, \boldsymbol{x}, \boldsymbol{x}') = \prod_{j=1}^{k} \exp\ [-\theta_{h;j}(x_j - x'_j)^2] = \exp\ [-\sum_{j=1}^{k} \theta_{h;j}(x_j - x'_j)^2], \quad (7)$$

which implies that the correlation between $o_h(\boldsymbol{x})$ and $o_h(\boldsymbol{x}')$ decreases exponentially, as $\boldsymbol{x}$ and $\boldsymbol{x}'$ are farther apart.

Because we use MATLAB *software* for SK (developed by Gonzalez—see Acknowledgment) to compute the predictor $\widehat{y}_h(\boldsymbol{x}_*)$ for a new point $\boldsymbol{x}_*$ and its estimated variance $s^2[\widehat{y}_h(\boldsymbol{x}_*)]$—given the old points $\boldsymbol{x}_i$ and the corresponding sufficient output statistics $\overline{o}_h(\boldsymbol{x}_i)$ and $s^2[\overline{o}_h(\boldsymbol{x}_i)]$ (defined in (5) and (6))—we present the exact formulas for $\widehat{y}_h(\boldsymbol{x}_*)$ and $s^2[\widehat{y}_h(\boldsymbol{x}_*)]$ in Appendix 1. Obviously, these $\boldsymbol{x}_i$ determine the $n \times k$ (deterministic) input matrix $\boldsymbol{X}$ and the n-dimensional (random) output vector $\overline{\mathbf{o}}_h(\boldsymbol{x}_i)$ and the diagonal covariance matrix for the intrinsic noise $\widehat{\boldsymbol{\Sigma}}_{\overline{e};h}$ with $s^2[\overline{o}_h(\boldsymbol{x}_i)]$. To compute $\widehat{\boldsymbol{\theta}}_h$ (in (7)), we must select a search area; we select the lower bound 0.001 and Gonzalez's upper bound $3^{1/2}$, for each $\theta_{h;j}$.

We let n_0 denote the *initial number of input combinations* of the input matrix $\boldsymbol{X}$. To select n_0, we follow Angün and Kleijnen (2023):

$$n_0 = (k+1)(k+2)/2 \text{ if } k \leq 6; \text{ else } n_0 = 5k. \quad (8)$$

Our (s, S) example has $k = 2$, so (8) gives $n_0 = 6$. Like most publications on Kriging, we use *Latin hypercube sampling* (LHS) to select a space-filling design with $\boldsymbol{l} \leq \boldsymbol{x} \leq \boldsymbol{u}$ (see (3)); like Angün and Kleijnen (2023) we use LHS *with midpoints*, so the n_0 points projected onto the k axes are equidistant (instead of clustered), which gives better $\widehat{\boldsymbol{\theta}}_h$. LHS with midpoints is an option in MATLAB's function *lhsdesign*.

Besides n_0, we must select m_0 which denotes the *initial number of replications for point* i with $i = 1, ..., n_0$. We start with $m_0 = 2$, which is the smallest value of m_0 that enables the computation of $s(o_h)$ (defined in (6)). Because our (s, S) model has a large simulation-runlength P, we expect a small $s(o_h)$ so $m_0 = 2$ might suffice.

Like Angün and Kleijnen (2023), we validate the SK models—estimated from the initial or pilot stage with n_0 input combinations—via the popular *leave-one-out cross-validation* (LOO-CV) test with prespecified error rate (say) α_{CV}. In our numerical experiment with an (s, S) model, we specify $\alpha_{\text{CV}} = 0.20$. LOO-CV means that we delete $\boldsymbol{x}_i$ (with $i = 1, ..., n_0$) and its $\overline{o}_h(\boldsymbol{x}_i)$ and $s^2[\overline{o}_h(\boldsymbol{x}_i)]$, and use the remaining simulation I/O data to compute $\widehat{y}_{-i;h}$ and $s^2(\widehat{y}_{-i;h})$, etc. We use the *Bonferroni* inequality with $2n_0$ CIs (because $i = 1, ..., n_0$ and our (s, S) model has two outputs), two-sided CIs (so we halve α_{CV}), and the *standard normal* variable z; i.e., we reject the SK models if

$$max_{i;h} \left[\frac{|\overline{o}_{i;h} - \widehat{y}_{-i;h}|}{\sqrt{s^2(\overline{o}_{i;h}) + s^2(\widehat{y}_{-i;h})}} \right] > z_{1-[\alpha_{\text{CV}}/(4n_0)]}. \quad (9)$$

If (9) holds, then we add a single replication to those points that require additional replications according to the following procedure.

Angün and Kleijnen (2023) applies *Law* (2005, p. 505)'s sequential procedure for estimating $E(o_h)$ with prespecified *relative error* γ (with $0 < \gamma < 1$) and prespecified *confidence level* $1 - \alpha_m$ (we use α_m, because we have already used α in $q_{1-\alpha}(w_1)$); in our experiment with an (s, S) model, we specify $\gamma = 0.10$ and $\alpha_m = 0.10$:

$$\widehat{m}_h = min\left[r \geq m : \frac{t_{r-1;1-\alpha_m/2} s_h(m)/\sqrt{r}}{|\overline{o}_h(m)|} \leq \frac{\gamma}{1+\gamma}\right], \tag{10}$$

where $s_h/\overline{o}_h$ is the *coefficient of variation* of output h. However, if $\overline{o}_h(m) \approx 0$, then (10) gives $\widehat{m}_h$ so high that we apply Law (2005, p. 504)'s procedure; i.e., in (10) we replace $\gamma/(1+\gamma)$ by the *absolute error* β and $|\overline{o}_h(m)|$ by the constant 1. Indeed, our (s, S) model tends to give $\widehat{\overline{q}}_{1-\alpha}[w_1(\boldsymbol{x})] \approx 0$ if $\boldsymbol{x}$ lies far away inside the feasible area so $w_{1;r}(\boldsymbol{x}) \approx 0$; we then specify $\beta = 0.01$.

Because the simulation model gives *multiple* types of output o_h, we apply (10)—possibly adapted for $\overline{o}_h(m) \approx 0$—such that this equation holds for all these outputs, at a given $\boldsymbol{x}$. So, the estimated *desired* number of replications at $\boldsymbol{x}$ is

$$\widehat{m}_i(\boldsymbol{x}) = \max_h \ [\widehat{m}_h(\boldsymbol{x})]. \tag{11}$$

Our *replication rule* stops adding replications for $\boldsymbol{x}$, as soon as $m_i \geq \widehat{m}_i$ holds.

After the initial stage with n_0 simulation input combinations, we also apply this replication rule to the one input combination that a next iteration selects as the new combination to be simulated; see the next section. (Chang and Cuckler (2022, Section 3.2) also discusses the selection of m in simulation optimization involving a quantile; Baker et al. (2022, Section 4) discusses the selection of n and m in the prediction of means and quantiles.)

3.4 EGO with KKT conditions

To solve our problem defined in (3), we apply Angün and Kleijnen (2023)'s algorithm which we call EGO-KKT. EGO is a popular method that uses Kriging and was originally developed for non-constrained optimization in deterministic simulation. Because the simulation-optimization problem may have multiple optima, EGO balances global search and local search—or exploration of the whole experimental area versus exploitation of a local promising area. EGO is sequential; i.e., it selects a *new* input combination $\boldsymbol{x}_*$ to be simulated next—given the n *old* (already simulated) combinations $\boldsymbol{x}_i$ with $i = 1, ..., n$ (in the initial stage, $n = n_0$; in the next stages n is updated one-by-one). To select $\boldsymbol{x}_*$, EGO's most popular criterion is the *infill criterion* or the *acquisition function* that uses the *expected improvement* (EI) which—in deterministic unconstrained minimization—is defined as

$$\text{EI}(\boldsymbol{x}_*) = E[max\ (w_{0;\,\min} - \widehat{y}(\boldsymbol{x}_*), 0)] \text{ with } w_{0;\,\min} = \min_{1 \leq i \leq n} [w_0(\boldsymbol{x}_i)]. \tag{12}$$

Jones et al. (1998) derives the following *estimator* $\widehat{\mathrm{EI}}_0(\boldsymbol{x}_*)$ where Φ and ϕ denote the CDF and the PDF of z:

$$\widehat{\mathrm{EI}}_0(\boldsymbol{x}_*) = (w_{0;\,\min} - \widehat{y}_0(\boldsymbol{x}_*))\,\Phi\left(\frac{w_{0;\,\min} - \widehat{y}_0(\boldsymbol{x}_*)}{s[\widehat{y}_0(\boldsymbol{x}_*)]}\right) + s[\widehat{y}_0(\boldsymbol{x}_*)]\phi\left(\frac{w_{0;\,\min} - \widehat{y}_0(\boldsymbol{x}_*)}{s[\widehat{y}_0(\boldsymbol{x}_*)]}\right).$$

If $s[\widehat{y}_0(\boldsymbol{x}_*)]$ is high, then $\widehat{\mathrm{EI}}_0(\boldsymbol{x}_*)$ stimulates exploration instead of exploitation.

For random simulation (such as our (s, S) simulation), Angün and Kleijnen (2023) uses the estimated *modified EI* (MEI):

$$\widehat{\mathrm{MEI}}(\boldsymbol{x}) = (\widehat{y}_{0;\,\min} - \widehat{y}_0(\boldsymbol{x}))\,\Phi\left(\frac{\widehat{y}_{0;\,\min} - \widehat{y}_0(\boldsymbol{x})}{s_{\mathrm{OK}}[\widehat{y}_0(\boldsymbol{x})]}\right) + s_{\mathrm{OK}}[\widehat{y}_0(\boldsymbol{x})]\phi\left(\frac{\widehat{y}_{0;\,\min} - \widehat{y}_0(\boldsymbol{x})}{s_{\mathrm{OK}}[\widehat{y}_0(\boldsymbol{x})]}\right). \tag{13}$$

To control the probability of selecting an *infeasible* solution, EGO-KTT uses a prespecified α_{infe} and accepts $\boldsymbol{x}$ as a feasible point only if in our experiment with an (s, S) model

$$\widehat{y}_1(\boldsymbol{x}) + z_{(1-\alpha_{\mathrm{infe}})} s[\widehat{y}_1(\boldsymbol{x})] \leq c_1. \tag{14}$$

In our experiment we select $\alpha_{\mathrm{infe}} = 1\%$ (so $z_{(1-\alpha)} = 2.3263$).

EGO-KKT *penalizes* $\widehat{\mathrm{MEI}}(\boldsymbol{x})$—where $\boldsymbol{x}$ satisfies (14)—if the *KKT conditions* do not hold at this $\boldsymbol{x}$ (as we shall see in (18)). These conditions use ∇_0 (gradient of $E[w_0(\boldsymbol{x})]$) and ∇_1 (gradient of $q_{1-\alpha}[w_1(\boldsymbol{x})]$)—provided the constraint for $q_{1-\alpha}[w_1(\boldsymbol{x})]$ holds (i.e., $\boldsymbol{x}$ lies on the boundary of the feasible area). These ∇_h ($h = 0, 1$) imply that $E[w_0(\boldsymbol{x})]$ and $q_{1-\alpha}[w_1(\boldsymbol{x})]$ are differentiable, so we assume that $F(w_1)$ (defined in (2)) is differentiable (i.e., $F(w_1)$ has no jumps or kinks).

The *black-box* simulation model implies that ∇_h and the boundary are unknown. Therefore, EGO-KKT estimates ∇_h via $\widehat{y}(\boldsymbol{x})$, which gives $\widehat{\nabla}_h(\boldsymbol{x}) = \nabla[\widehat{y}_h(\boldsymbol{x})] = (\partial[\widehat{y}_h(\boldsymbol{x})]/\partial x_j)'$. Defining $\tau_h^2 = Var(y_h)$, Angün and Kleijnen (2023) derives that (7) gives

$$\frac{\partial[\widehat{y}_h(\boldsymbol{x})]}{\partial x_j} = -2\widehat{\tau}_h^2\widehat{\theta}_{h;j}\{\Sigma_{i=1}^n c_{h;i}(x_{*;j} - x_{i;j})\exp[\Sigma_{j'=1}^k - \widehat{\theta}_{h;j'}(x_{*;j'} - x_{i;j'})^2]\}. \tag{15}$$

Furthermore, EGO-KKT estimates that the output constraint is *binding* at $\boldsymbol{x}$ if the following two-sided CI with prespecified α_{BC} (where BC stands for "binding constraint") holds:

$$\frac{|\widehat{y}_1(\boldsymbol{x}) - c_1|}{s[\widehat{y}_1(\boldsymbol{x})]} \leq z_{1-\alpha_{\mathrm{BC}}/2}. \tag{16}$$

Because in our (s, S) simulation, the input bounds $\boldsymbol{l}$ and $\boldsymbol{u}$ in (3) are rather arbitrary, we assume that the *input constraints* are not binding when searching

for $\boldsymbol{x}$ (if input constraints are binding, then Angün and Kleijnen (2023) extends the KKT conditions).

Letting the symbol $\widetilde{}$ denote *least squares* (LS) estimators, we obtain the following LS estimator of the *Lagrange multiplier*:

$$\widetilde{\lambda}_1(\boldsymbol{x}) = [\widehat{\nabla}_1(\boldsymbol{x})'\widehat{\nabla}_1(\boldsymbol{x})]^{-1}\widehat{\nabla}_1(\boldsymbol{x})'[-\widehat{\nabla}_0(\boldsymbol{x})].$$

This $\widetilde{\lambda}_1(\boldsymbol{x})$ gives the following LS model with the explained (dependent) variable $-\widetilde{\nabla}_0(\boldsymbol{x})$ and the explanatory (independent) variable $\widehat{\nabla}_1(\boldsymbol{x})$ that models the *KKT stationarity conditions*:

$$-\widetilde{\nabla}_0(\boldsymbol{x}) = \widetilde{\lambda}_1(\boldsymbol{x})\widehat{\nabla}_1(\boldsymbol{x})] \text{ with } \widetilde{\lambda}_1(\boldsymbol{x}) \geq 0.$$

To quantify how well these conditions hold, Angün and Kleijnen (2023) computes the *angle* between $\widehat{\nabla}[\widehat{y}_0(\boldsymbol{x})]$ and $\widetilde{\nabla}[\widehat{y}_0(\boldsymbol{x})]$. It is well known that this angle is measured by the following cosine where $\bullet$ denotes the inner product of two vectors and $||\ ||$ denotes the l_2-norm:

$$\widetilde{\cos}(\boldsymbol{x}) = \frac{\widehat{\nabla}[\widehat{y}_0(\boldsymbol{x})] \bullet \widetilde{\nabla}[\widehat{y}_0(\boldsymbol{x})]}{||\widehat{\nabla}[\widehat{y}_0(\boldsymbol{x})]|| \times ||\widetilde{\nabla}[\widehat{y}_0(\boldsymbol{x})]||}. \tag{17}$$

Ideally, $\widehat{\nabla}[\widehat{y}_0(\boldsymbol{x})]$ and $\widetilde{\nabla}[\widehat{y}_0(\boldsymbol{x})]$ point into exactly the same direction so their angle is zero and $\widetilde{\cos}(\boldsymbol{x}) = 1$.

Altogether, EGO-KKT tries to find $\widehat{\boldsymbol{x}}_{\text{o}}$ (estimated optimal $\boldsymbol{x}$) that maximizes the infill criterion:

$$\widehat{\boldsymbol{x}}_{\text{o}} = \arg\ [\max_{\boldsymbol{x}} \widehat{\text{MEI}}(\boldsymbol{x}) \times \widetilde{\cos}(\boldsymbol{x})] \tag{18}$$

where $\boldsymbol{x}$ in $\widetilde{\cos}(\boldsymbol{x})$ lies within the two-sided CI for the *binding constraint* in (16),

and the search is limited to the estimated *feasible area* defined by the one-sided CI in (14).

To find this $\widehat{\boldsymbol{x}}_{\text{o}}$, EGO-KKT uses MATLAB's function for finding the minimum of a constrained problem—called *fmincon*. Because fmincon is a local optimizer, we use $n_{\text{fmincon}} > 1$ starting points; for our (s, S)model we select $n_{\text{fmincon}} = 20$. To sample these n_{fmincon} points in $\boldsymbol{l} \leq \boldsymbol{x} \leq \boldsymbol{u}$, we apply LHS without midpoints. Because fmincon requires a *feasible* starting point, we use only feasible points among these n_{fmincon} points. For further details on the use of fmincon in EGO-KKT, we refer to Angün and Kleijnen (2023).

After finding $\widehat{\boldsymbol{x}}_{\text{o}}$ (solving (18) with its constraints), EGO-KKT obtains *replications* for $\widehat{\boldsymbol{x}}_{\text{o}}$—applying (11). EGO-KKT *terminates* when it satisfies a prespecified stopping criterion; in our experiments, it terminates after 95 iterations. More details of EGO-KKT are given in Angün and Kleijnen (2023), including a pseudo-code for EGO-KKT.

4 Numerical example: a specific (s, S) model

For our numerical experiment, we use a PC with multiple cores and parallel software that enable 12 restarts of EGO-KKT such that each restart samples

its own initial design. Such parallel computing implies that the restarts do not increase *wall-clock time*. Within each of these restarts, we use 20 non-parallel restarts of fmincon.

In our specific (s, S) discrete-event simulation, demand D is exponentially distributed with mean 100, and lead time L is integer-valued Poisson distributed with mean 6. The basic sequence of events in each period p is as follows: Orders are received at the beginning of the period, the demand for the period is subtracted, then an order review is carried out.

To quantify the consequences of risk aversion, we compare the results of an (s, S) simulation model with a constraint for the expected disservice level (also studied in Angün and Kleijnen (2023)) and our inventory simulation. In Section 1 we have already mentioned that risk-aversion—modeled through a "high" quantile such as $q_{0.90;1}$—implies that s and S change. Now we add that obviously s and S increase, so we should explore an experimental area with higher maximum values for s and S. Therefore we now keep the same minimum value for s as Angün and Kleijnen (2023) uses; namely, $s_{\min} = 600$. For the maximum of s we select $s_{\max} = 2{,}400$ (instead of 1,200). Furthermore, besides $x_1 = s$ we define $x_2 = Q = S - s$. To select the bounds for Q, we again use the *economic order quantity* (EOQ), which equals 85. We vary Q between EOQ/8 = 10.625 and 8×EOQ = 680, Altogether, we use the box constraints $600 \leq s \leq 2{,}400$ and $10.625 \leq Q \leq 680$.

Table 1: Initial design for s and Q with $S = s + Q$ in restart 1 of macroreplication 1, with its average outputs $\overline{w}_0$ and $\overline{\widehat{q}}_{0.90;1}$ and their estimated standard deviations s; * denotes $\overline{\widehat{q}}_{0.90;1}(\mathbf{x}_i)$ significantly higher than $c_1 = 0.1$; number of replications m

s	Q	$S = s + Q$	$\overline{w}_0$	$s(\overline{w}_0)$	$\overline{\widehat{q}}_{0.90;1}$	$s(\overline{\widehat{q}}_{0.90;1})$	m
1950	66.4	2016.4	1423.3	0.9682	0.0014	0.0002	14
1650	624.2	2274.2	1412.1	1.2475	0.0044	0.0005	14
2250	178.0	2428.0	1787.3	0.9550	0.0000	0.0000	3
1350	289.5	1639.5	943.0	1.7477	0.0277	0.0015	4
750	401.1	1151.1	483.8	0.7007	0.2970*	0.0058	3
1050	512.7	1562.7	777.4	5.0430	0.0890	0.0046	3

As we discussed in Section 3.3, we *initially* select $n = 6$ for $\boldsymbol{X}_{n\times k}$, and $m_0 = 2$. Columns 1 and 2 of Table 1 display an example of $\boldsymbol{X}_{6\times 2}$ selected through LHS-with-midpoints of s and Q (so $S = s + Q$ in column 3) in restart 1 of macroreplication 1; e.g., $n = 6$ and $600 \leq s \leq 2{,}400$ implies that the smallest midpoint for s is 750 (see cell (5,1)). Columns 4 and 5 display $\overline{w}_0$ and $s(\overline{w}_0)$, computed from m replications per (s, S) combination. Likewise, columns 6 and 7 display $\overline{\widehat{q}}_{0.90;1}$ and $s(\overline{\widehat{q}}_{0.90;1})$, which determine a one-sided CI such that the symbol * denotes a $\overline{\widehat{q}}_{0.90;1}$-value that is significantly higher than $c_1 = 0.10$. Actually, $\alpha_m = 0.10$ implies that $\overline{\widehat{q}}_{0.90;1}$ is significantly higher than

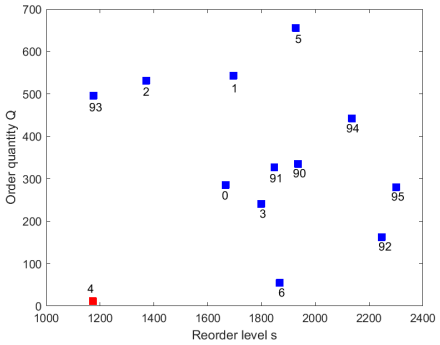

Figure 2: Example of trajectory's first and last iterations in the search for $(\widehat{s}_{\rm o}, \widehat{S}_{\rm o})$ where integers identify the iteration

c_1, in combination 5, which has the lowest s and S. This combination also gives the lowest $\overline{w}_0$ (low s and S implies low average inventory) The other five combinations give low $\overline{\widehat{q}}_{0.90;1}$-values, so they are points inside the feasible area. The last column displays m, which depends on $s_h/\overline{o}_h$; e.g., the combinations 1 and 6 give $s_1/\overline{o}_1$ equal to 0.0002/ 0.0014 = 0.14 and 0.0046/ 0.0890 = 0.05 so m equals 14 and 3 respectively. Combination 3 gives $\overline{\widehat{q}}_{0.90;1} = 0.0000$, so we use the absolute error $\beta = 0.01$ instead of γ.

After this initial design—or iteration 0—the EGO-KKT algorithm estimates the *optimal* point $(\widehat{s}_{\rm o}, \widehat{S}_{\rm o})$ and the corresponding optimal outputs $\overline{w}_0$ and $\overline{\widehat{q}}_{0.90;1}$; see the *trajectory* of the search for $(\widehat{s}_{\rm o}, \widehat{S}_{\rm o})$ in Fig. 2, which displays $(\widehat{s}_{\rm o}, \widehat{Q}_{\rm o})$ (so $\widehat{S}_{\rm o} = \widehat{s}_{\rm o} + \widehat{Q}_{\rm o}$) for the initial design, the first six iterations, and the last six iterations for restart 2 of macroreplication 1. We select this restart because it is one of the few trajectories that includes a point that is estimated to be infeasible upon actual simulation. We (rather arbitrarily) decided to stop the search for the (unknown) true optimum, after 95 iterations. In each iteration, the algorithm selects a new point $\widehat{\boldsymbol{x}}_{\rm o}$ that it estimates to be optimal. However, after actual simulation, the algorithm may estimate (via (14)) that $\widehat{\boldsymbol{x}}_{\rm o}$is infeasible—see iteration 4 (colored read; plots use color in the PDF file)—so it does not change the estimated optimal input $\widehat{\boldsymbol{x}}_{\rm min} = (\widehat{s}_{\rm o}, \widehat{Q}_{\rm o})$. If the algorithm estimates $\widehat{\boldsymbol{x}}_{\rm o}$to be feasible, then it may estimate that this $\widehat{\boldsymbol{x}}_{\rm o}$ does or does not give a better $\widehat{\boldsymbol{x}}_{\rm min}$; i.e., $\overline{w}_0(\widehat{\boldsymbol{x}}_{\rm min})$ decreases or stays the same as in the previous iteration. Because we do not know the true I/O functions $w_h(\boldsymbol{x})$, we cannot display the boundary of the feasible area in the plot; iteration 4 does confirm that too small values for $\widehat{s}_{\rm o}$ and $\widehat{Q}_{\rm o}$ do not satisfy the service-level constraint.

Appendix 2 displays a plot for m for each of the 95 iterations in one macroreplication, for the two alternative constraints This plot shows that the smallest m is 3 and the highest m is14 (these values also appear in the pilot stage displayed in Table .1, which samples the experimental area uniformly). As we expected, the $q_{0.90}(w_1)$ constraint more often requires 14 replications. In total, the 95 iter-

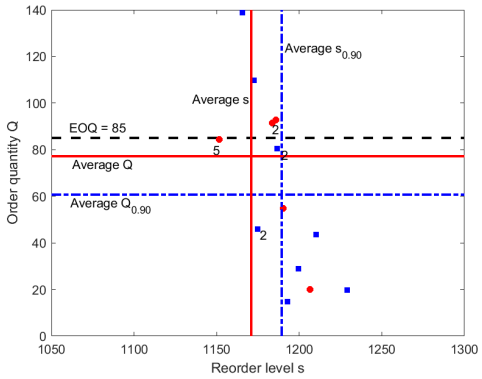

Figure 3: Final $(\widehat{s}_{\rm o}, \widehat{Q}_{\rm o})$ with either $E[w_1(\boldsymbol{x})] \leq 0.1$ (red balls) or $q_{0.90}[w_1(\boldsymbol{x})] \leq 0.1$ (blue squares); lines denote averages

ations for the $q_{0.90}(w_1)$ constraint require 709 simulation observations, whereas the $E(w_1)$ constraint requires 449 observations; i.e., on average, the $q_{0.90}(w_1)$ constraint increases m by 58%.

Next we decide to obtain $R = 10$ macroreplications, which sample different $\boldsymbol{X}_{6\times 2}$ (so the smallest midpoint for s is likely to be combined with a midpoint for Q that is not displayed in Table 1). We do not display the resulting Tables, but only mention that all combinations require $m > m_0 = 2$ (because $s(\widehat{\widehat{q}}_{0.90;1})$ is relatively high).

Fig. 3 displays $(\widehat{s}_{\rm o}, \widehat{Q}_{\rm o})$ for the $E[w_1(\boldsymbol{x})]$ constraint (red balls) and for the $q_{0.90;1}$ constraint (blue squares), respectively, after 95 iterations for each of the 10 macroreplications. Given the scale of the plot, some $(\widehat{s}_{\rm o}, \widehat{Q}_{\rm o})$ combinations coincide; e.g., "5" means that five combinations coincide for the $E[w_1(\boldsymbol{x})]$ constraint. The *average* values of $\widehat{s}_{\rm o}$ and $\widehat{Q}_{\rm o}$ are displayed by lines. This plot shows that the $q_{0.90;1}$ constraint gives a higher average for $\widehat{s}_{\rm o}$. This higher $\overline{\widehat{s}}_{\rm o}$ implies that the inventory level remains relatively high during the P simulated periods. Because the total demand during these P periods remains constant, $\overline{\widehat{Q}}_{\rm o}$ decreases; i.e., smaller orders are placed more frequently. Furthermore, when the constraint changes, $\widehat{s}_{\rm o}$ and $\widehat{Q}_{\rm o}$ do not change much—given the scale of the plot (the total experimental area is defined by $600 \leq s \leq 2{,}400$ and $10.625 \leq Q \leq 680$). However, the key question is whether changes in $\widehat{s}_{\rm o}$ and $\widehat{Q}_{\rm o}$ have large effects on the cost and service level; we answer this question next.

Fig. 3 gives Fig. 4, which displays the estimated disservice level versus cost. This plot shows that the average values of the disservice measures $\overline{w}_1$ and $\overline{\widehat{q}}_{0.90;1}$ are close to their (common) threshold 0.10, and these values are nearly the same; i.e., our algorithm searches for the constrained optimum, and finds it near the boundary of the feasible area (this algorithm stays on the "safe" side of the constraint; see $\alpha_{\rm infe} = 1\%$ in (14)). This plot also shows that the average cost $\overline{w}_0$ is higher for the $q_{0.90}[w_1(\boldsymbol{x})]$ constraint than it is for the $E[w_1(\boldsymbol{x})]$

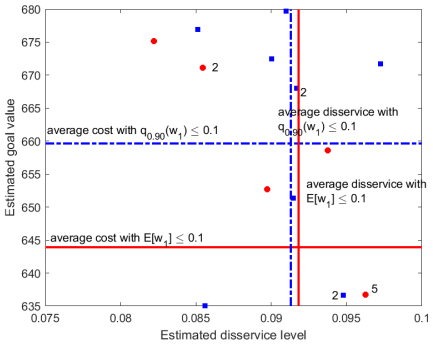

Figure 4: Final $(\widehat{\overline{q}}_{0.90;1}, \overline{w}_0)$ with $E[w_1(\boldsymbol{x})] \leq 0.1$ (red balls), $q_{0.90}[w_1(\boldsymbol{x})] \leq 0.1$ (blue squares); lines denote averages

constraint; Appendix 3 gives the precise values, which imply that $\overline{w}_0$ is 2.4% higher (namely, (659.7 - 643.9)/643.9 = 0.024). This 2.4% increase may be prohibitive in supermarket inventory management with its small profit margin. This appendix also details our statistical analysis of Fig. 4, which shows that $\overline{w}_0$ for the $q_{0.90}[w_1(\boldsymbol{x})]$ constraint is *significantly* higher if we use a type-I error rate of 10% or 5% (not 1%).

5 Conclusions and future research

In this paper we investigated the cost of risk-aversion in an inventory system that is controlled by an (s, S) model with parameters specified in Bashyam and Fu (1998). We defined risk-aversion as the requirement that the 90% quantile—instead of the expected value—of the disservice level remain below 0.10. To estimate the values of the decision variables s and S that satisfy this service-level constraint while minimizing the expected inventory cost, we apply Angün and Kleijnen (2023)'s algorithm that combines EGO with the KKT conditions. Our numerical results show that the risk-averse requirement increases cost by 2.4%. It is up to management to decide whether this cost increase is acceptable.

In future research, we may investigate epistemic uncertainty (besides aleatory uncertainty). Parmar et al. (2022) investigates this uncertainty—but not in the context of optimization. Wauters (2024) investigates epistemic and aleatory uncertainties in robust optimization.

Acknowledgement

We use the MATLAB code for stochastic Kriging developed by Sebastian Rojas Gonzalez, former FWO Postdoctoral Fellow, Hasselt University and Ghent University, while he was a Ph.D. student at KU Leuven, Belgium. We re-

ceived useful comments on the various definitions of service levels from Jan C. Fransoo, Professor of Operations and Logistics Management, Tilburg School of Economics and Management, Tilburg University.

References

Alexopoulos, C., D. Goldsman, A.C. Mokashi, K-W. Tien, and J.R. Wilson (2019), Sequest: a sequential procedure for estimating quantiles in steady-state simulations. *Operations Research*, 67, no. 4, pp. 1162–1183

Angün, E. and J. Kleijnen (2023). Constrained optimization in random simulation: efficient global optimization and Karush-Kuhn-Tucker conditions. Submitted for publication (Preprint: CentER Discussion Paper 2023-010 https://www.tilburguniversity.edu/research/economics-and-management/publications/discussion-paper)

Ankenman,B., B. Nelson, and J. Staum (2010) Stochastic kriging for simulation metamodeling. *Operations Research*, 58, no. 2, pp. 371–382

Baker, E., P. Barbillon, A. Fadikar, R.B. Gramacy, R. Herbei, D. Higdon, J. Huang, L.R. Johnson, P. Ma, A. Mondal, B. Pires, J. Sacks, and V. Sokolov (2022), Analyzing stochastic computer models: a review with opportunities. *Statistical Science*, 37, no. 1, pp. 64–89. DOI: 10.1214/21-STS822

Bashyam, S. and M.C. Fu (1998) Optimization of (s, S) inventory systems with random lead times and a service level constraint. *Management Science*, 44, pp. 243–256

Chang, K.H. (2015),. A direct search method for unconstrained quantile-based simulation optimization. *European Journal of Operational Research*, 246, no. 2, pp. 487–495

Chang, K.H. (2016a), Risk-controlled product mix planning in semiconductor manufacturing using simulation optimization. *IEEE Transactions on Semiconductor Manufacturing*, 29, no. 4, pp. 411–418

Chang, K.H. (2016b), A quantile-based simulation optimization model for sizing hybrid renewable energy systems. *Simulation Modelling Practice and Theory*, 66, pp. 94–103

Chang, K.H. and R. Cuckler (2022), Applying simulation optimization for agile vehicle fleet sizing of automated material handling systems in semiconductor manufacturing. *Asia-Pacific Journal of Operational Research*, 39, no. 2 2150018 (22 pages) DOI: 10.1142/S0217595921500184

Chang, K.H. and C.P. Lin (2023), An efficient simulation optimization method for the redundancy allocation problem with a chance constraint. *Journal of the Operational Research Society*, DOI: 10.1080/01605682.2023.2272860

Chang, K.H. and H.K. Lu (2016), Quantile-based simulation optimization with inequality constraints: methodology and applications. *IEEE Transactions on Automation Science and Engineering*, 13, no. 2, pp. 701–708

Coelho, G.F. and L.R. Pinto (2018) Kriging-based simulation optimization: An emergency medical system application. *Journal of the Operational Research Society*, 69, no. 12, 2006-2020, DOI: 10.1080/01605682.2017.1418149

Hu, J.,Y. Peng, G. Zhang, and Q. Zhang (2022), A stochastic approximation method for simulation-based quantile optimization. *INFORMS Journal on Computing*, 34, no. 6, pp. 2889–2907

Jones, D., M. Schonlau, and W. Welch (1998). Efficient global optimization of expensive blackbox functions. *Journal of Global Optimization*, 13, pp. 455–492

Kleijnen, J.P.C. (2015), *Design and analysis of simulation experiments; second edition*. Springer

Kleijnen, J.P.C., E. Angün, I. van Nieuwenhuyse, and W.C.M. van Beers (2023), Constrained optimization in simulation: efficient global optimization and Karush-Kuhn-Tucker conditions. Submitted for publication (Preprint: CentER Discussion Paper 2022-015

https://pure.uvt.nl/ws/portalfiles/portal/62445340/2022_015.pdf)

Law, A.M. (2015), *Simulation modeling and analysis; fifth edition*. McGraw-Hill, Boston

Lolos, A., C. Alexopoulos, D. Goldsman, K.D. Dingeç, A.C. Mokashi, and J.R. Wilson (2023), A fixed-sample-size method for estimating steady-state quantiles. *Proceedings of the 2023 Winter Simulation Conference*, edited by C.G. Corlu, S.R. Hunter, H. Lam, B.S. Onggo, J. Shortle, and B. Biller, in press

Lu, C. and J.A. Paulson (2023), No-regret constrained Bayesian optimization of noisy and expensive hybrid models using differentiable quantile function approximations. arXiv:2305.03824v2 [stat.ML] 28 Jul 2023

Maitra, S. (2024), A System-dynamic based simulation and Bayesian Optimization for inventory management. arXiv preprint arXiv:2402.10975

Ouyang, L., M. Han, Y. Ma, M. Wang, and C. Park (2023) Simulation optimization using stochastic kriging with robust statistics. *Journal of the Operational Research Society*, 74:3, 623-636, DOI: 10.1080/01605682.2022.205549

Parmar, D., L.E.. Morgan, S.M. Sanchez, A.C. Titman, and R.A. Williams (2022), Input uncertainty quantification for quantiles. *Proceedings of the 2022 Winter Simulation Conference*, edited by B. Feng, G. Pedrielli, Y. Peng, S. Shashaani, E. Song, C.G. Corlu, L.H. Lee, E.P. Chew, T. Roeder, and P. Lendermann, pp. 97–108

Song, E., H. Lam, and R.R. Barton (2024), A shrinkage approach to improve direct bootstrap resampling under input uncertainty. *INFORMS Journal on Computing*, in press

Wang, S., S.H. Ng, and W.B. Haskell (2022) A multilevel simulation optimization approach for quantile functions. *INFORMS Journal on Computing*, 34, no. 1, pp. 569–585

Wauters, J. (2024), ERGO-II: an improved Bayesian optimization technique for robust design with multiple objectives, failed evaluations and stochastic parameters. *Journal of Mechanical Design*, doi:10.1115/1.4064674

Appendix 1: Stochastic Kriging: predictor and variance formulas

Let M_h denote the extrinsic noise of output h. Kriging assumes that M_h is independent of the intrinsic noise e_h. This M_h has the mean $\mu_h = E(y_h)$ and the variance $\tau_h^2 = Var(y_h)$, so the correlation matrix $\mathbf{R}_h = (\rho_{i;i';h})$ equals $\tau_h^{-2}\mathbf{\Sigma}_{M;h}$ with the covariance matrix $\mathbf{\Sigma}_{M;h} = (\text{Cov}(y_{h;i}, y_{h;i'}))$ where $y_{h;i} = y_h(\boldsymbol{x}_i)$ and $i' = 1, ..., n$. The correlations between the Kriging outputs of type h at the *new* point $\boldsymbol{x}_*$ and the n old points are $\boldsymbol{\rho}_h(\boldsymbol{x}_*) = \tau_h^{-2}\boldsymbol{\sigma}_{M;h}(\boldsymbol{x}_*)$ with the n-dimensional covariance vector $\boldsymbol{\sigma}_{M;h}(\boldsymbol{x}_*) = (\sigma_{h;*}) = (\text{Cov}(y_{h;*}, y_{h;i})$ with $y_{h;*} = y_h(\boldsymbol{x}_*)$. Like most publications on SK, we assume *constant* means $\mu_h = E(y_h)$ (so we use OK) instead of low-order polynomials in $\boldsymbol{x}$ (assumed in universal Kriging). Finally, $\mathbf{1}_n$ denotes the n-dimensional vector with all elements equal to 1. Like most publications on Kriging (including SK), we use the *maximum likelihood estimator* (MLE) for the parameters of the extrinsic noise and the unbiased estimators for the intrinsic noise; we let the symbol $\widehat{}$ denote these MLEs and unbiased estimators. Using these symbols, SK gives the predictor

$$\widehat{y}_h(\boldsymbol{x}_*) = \widehat{\mu}_h + \widehat{\boldsymbol{\sigma}}_{M;h}(\boldsymbol{x}_*)'(\widehat{\mathbf{\Sigma}}_{M;h} + \widehat{\mathbf{\Sigma}}_{\overline{e};h})^{-1}(\overline{\mathbf{o}}_h - \widehat{\mu}_h\mathbf{1}_n), \tag{19}$$

and

$$s^2[\widehat{y}_h(\boldsymbol{x}_*)] = \widehat{\tau}_h^2 - \widehat{\tau}_h^4\boldsymbol{\rho}_h'(\boldsymbol{x}_*)[\widehat{\tau}_h^2\mathbf{R}_h + \widehat{\mathbf{\Sigma}}_{\overline{e};h}]^{-1}\boldsymbol{\rho}_h(\boldsymbol{x}_*) + \widehat{\delta}_h^2[\mathbf{1}_n'(\widehat{\tau}_h^2\mathbf{R}_h + \widehat{\mathbf{\Sigma}}_{\overline{e};h})^{-1}\mathbf{1}_n]^{-1}$$
$$\text{with } \widehat{\delta}_h = 1 - \mathbf{1}_n'(\widehat{\tau}_h^2\mathbf{R}_h + \widehat{\mathbf{\Sigma}}_{\overline{e};h})^{-1}\boldsymbol{\rho}_h(\boldsymbol{x}_*)\widehat{\tau}_h^2. \tag{20}$$

The modified EI (MEI) also uses s_{OK}^2, which denotes the estimated variance of the OK predictor; obviously, s_{OK}^2 equals $s[\widehat{y}_h(x_*)]$ after deleting $\widehat{\mathbf{\Sigma}}_{\overline{e};h}$ in **(20).**

If the Gaussian correlation function is selected, then M_h is specified by the parameter vector $\boldsymbol{\psi}_h = (\mu_h, \tau_h^2, \theta_{h;1}, ..., \theta_{h;k})'$. The MLE of $\boldsymbol{\psi}_h$ is denoted by $\widehat{\boldsymbol{\psi}}_h$.

Appendix 2: Number of replications per iteration

Fig. 5 displays m for the two alternative constraints, for each of the 95 iterations in a specific macroreplication.

Appendix 3: Statistical analysis of numerical results for (s, S) model

Fig. 6 displays the scatterplot of $\overline{w}_{0;r}$ in $(\overline{w}_{1;r}, \overline{w}_{0;r})$ versus $\overline{w}_{0;r}$ in $(\overline{\widehat{q}}_{0.90;1;r}, \overline{w}_{0;})$ in $R = 10$ macroreplications; i.e., the main text displays a plot with the final $(\overline{w}_{1;r}, \overline{w}_{0;r})$ (using $E[w_1(\boldsymbol{x})] \leq 0.1$) and the final $(\overline{\widehat{q}}_{0.90;1;r}, \overline{w}_{0;r})$ (using the constraint $q_{0.90;1} \leq 0.1$) for macroreplication r with $r = 1, ..., R$. Obviously, the two constraints given different observations on $\overline{w}_0$. In a given macroreplication r for the two constraints, we use the same PRN seed to start the search for the optimum during 95 iterations. However, we do not try to synchronize the PRN streams with the same seed, so these streams get out-of-step because the $q_{0.90;1}$ constraint tends to require more replications than the $E(w_1)$ constraint does; see Fig. 5. Therefore we hypothesize that the observations on $\overline{w}_0$ for the

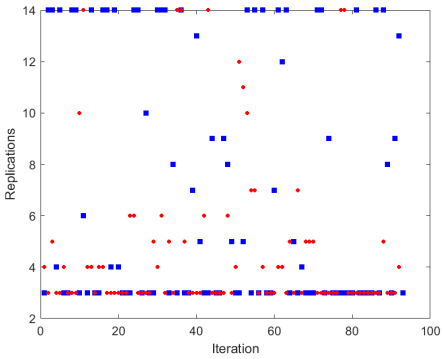

Figure 5: Number of replications m per iteration in a specific macroreplication; red balls correspond with the $E(w_1)$ constraint and blue squares with the $q_{0.90}(w_1)$ constraint

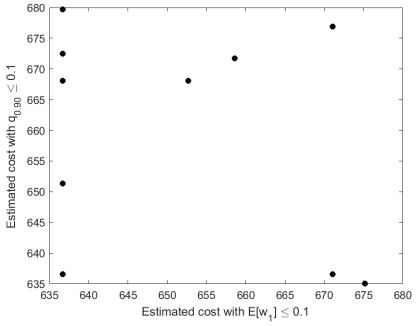

Figure 6: Scatterplot of $\overline{w}_{0;r}$ in $(\overline{w}_{1;r}, \overline{w}_{0;r})$ versus $\overline{w}_{0;r}$ in $(\widehat{\overline{q}}_{0.90;1;r}, \overline{w}_{o;r})$ with $r = 1, ..., 10$

two constraints in the same macroreplication are only weakly correlated; see the *scatterplot* in Fig. 6. (This scatterplot has five observations on $\overline{w}_0$ for the $E(w_1)$ constraint that are very close to 635, which agrees with plot in the main text.) Let $\overline{w}_{0;E}$ and $\overline{w}_{0;q_{0.90}}$ denote $\overline{w}_{\text{o}}$ when using the constraint $E[w_1(\boldsymbol{x})] \leq 0.1$ and $q_{0.90;1} \leq 0.1$, respectively. We denote the *estimated correlation coefficient* for $(\overline{w}_{0;E},\overline{w}_{0;q_{0.90}})$ by $\widehat{\rho}(\overline{w}_{0;E},\overline{w}_{0;q_{0.90}})$ or briefly $\widehat{\rho}_0$. The data that give Fig. 6, also give $\widehat{\rho}_0 = -0.1965$. To *test* the null-hypothesis H_0: $E(\widehat{\rho}_0) = 0$, we use the well-known formula

$$t_{R-2} = \widehat{\rho}_0 \times \sqrt{\frac{R-2}{1-\widehat{\rho}_0^2}} \tag{21}$$

which gives $t_8 = -0.1965 \times [8/(1-0.1965^2)]^{1/2} = -0.5668$. So if the alternative hypothesis is H_1: $E(\widehat{\rho}_0) > 0$ (because of the expected effect of CRN), then $p = PR(t_8 > -0.5668) = 0.7068$ so—for any usual value of the *type-I error rate* (say) α_{I}—we do not reject $E(\widehat{\rho}_0) = 0$ in favor of $E(\widehat{\rho}_0) > 0$. If H_1: $E(\widehat{\rho}_0) \neq 0$, then $p = 2 \times PR(t_8 < -0.5668) = 2 \times 0.2932 = 0.5864$, so we again do not reject $E(\widehat{\rho}_0) = 0$.

To test whether $\overline{w}_{0;q_{0.90}}$and $\overline{w}_{0;E}$ have different expected values, we might use the *paired* t statistic (even though (21) does not reject $E(\widehat{\rho}_0) = 0$):

$$t_{R-1}(q_{0.90}) = \frac{\overline{d}}{s_{\overline{d}}} \text{ with } d_r = \overline{w}_{0;q_{0.90};r} - \overline{w}_{0;E;r}, \tag{22}$$

which gives $15.7089/7.5083 = 2.0922$ so $p = PR(t_9 > 2.0922) = 0.0330$ so for $\alpha_{\text{I}} = 10\%$ or $\alpha_{\text{I}} = 5\%$ we "accept" $E(d) > 0$ or $E(\overline{w}_{0;q_{0.90}}) > E(\overline{w}_{0;E})$ (for $\alpha_{\text{I}} = 1\%$ we do not reject $E(d) = 0$).

Instead of (22) we may use the *two-sample* t statistic, assuming that $\overline{w}_{0;q;r}$ and $\overline{w}_{0;E;r}$ are independent and have equal variances ($\sigma^2(\overline{w}_{0;q_{0.90}}) = \sigma^2(\overline{w}_{0;E})$) so we pool the estimated variances, which doubles the degrees of freedom:

$$t_{2R-2}(q_{0.90}) = \frac{\overline{\overline{w}}_{0;q_{0.90}} - \overline{\overline{w}}_{0;E}}{\sqrt{s^2(\overline{\overline{w}}_{0;q_{0.90}}) + s^2(\overline{\overline{w}}_{0;E})}}, \tag{23}$$

which gives $(659.6536-643.9447)/(32.1001+15.5054)^{1/2} = 2.2768$ so $p = PR(t_{18} > 2.2768) = 0.0176$, so $\alpha_{\text{I}} = 10\%$ or $\alpha_{\text{I}} = 5\%$ implies that we "accept" $E(\overline{w}_{0;q_{0.90}}) > E(\overline{w}_{0;E})$.